International Journal of Modern Physics D
Vol. 25, No. 13 (2016) 1645013 (11 pages)

DOI: 10.1142/S0218271816450139

Design and implementation of the TAROGE experiment

J. W. Nam*,‡, C.-C. Chen*, C.-H. Chen*, C.-W. Chen*, P. Chen*, Y.-C. Chen*, S.-Y. Hsu*, J.-J. Huang*, M.-H. A. Huang†, T.-C. Liu*, J. Řípa*, Y.-S. Shiao*, M.-Z. Wang* and S.-H. Wang*

*Department of Physics, Institute of Astrophysics, and Leung Center for Cosmology and Particle Astrophysics, National Taiwan University, Sec. 4 No. 1. Roosevelt Road, Taipei 10617, Taiwan

†Department of Energy and Resources, National United University, 2 Lianda Road, Miao-Li 36003, Taiwan

‡jwnam@phys.ntu.edu.tw

Received 25 May 2016
Accepted 3 May 2016
Published 20 July 2016

Taiwan astroparticle radiowave observatory for geo-synchrotron emissions (TAROGE) is an antenna array on the high mountains of Taiwan's east coast for the detection of ultra-high energy cosmic rays (UHECRs) in an energy above $10^{18.5}$ eV. The antennas point toward the ocean to detect radiowave signals emitted by the UHECR-induced air-shower as a result of its interaction with the geomagnetic field. Looking down from the coastal mountain, the effective area is enhanced by collecting both direct-emission as well as the ocean-reflected signals. This instrument also provides the capability of detecting earth-skimming tau-neutrino through its subsequent tau-decay induced shower. In order to prove the detection concept, initial two stations were successfully built at 1000 m elevation near Heping township, Taiwan, in 2014–2015. Each station consists of 12 log-periodic dipole array antennas for 110–300 MHz. The stations have been operating smoothly for radio survey and optimization of instrumental parameters. In this report, we discuss the design of TAROGE, the performance of the prototype station and the future prospect.

Keywords: Ultra-high energy cosmic rays; extensive air showers; radio detection.

PACS Number(s): 96.50.sd, 07.57.Kp, 84.40.−x

1. Introduction

The radio detection method has recently been established as a promising alternative solution for detecting of ultra-high energy cosmic rays (UHECRs) which is challenging due to the extremely low flux. It would require a detection area several orders of magnitude larger than the current largest cosmic ray detector; Pierre Auger Observatory,[1] to identify their astrophysical sources. Radio emission from

extensive air showers is a form of geo-synchrotron radiation, which arises from the deflection of electrons and positions in the shower by the Earth magnetic field. Such radiations at radio-band are coherently added during air-shower development because the radio wavelengths are longer than the shower size, which results in intense pulses that can be detected at a distance of several hundred kilometers. Therefore, one can effectively cover a huge detection area with a small number of radio antennas. Furthermore, the radio detection system can be operated all year round and day-and-night, which leads to a duty cycle as high as ∼100%. Several frontier experiments such as LOPES, ANITA, and AREA[2–4] have demonstrated powerful capability of the radio detection method for UHECRs. For instance, the ANITA experiment, a NASA balloon-borne antenna array that surveys Antarctica from the altitude of 35 km, reported the observation of 16 events with averaged energy $\langle E \rangle = 1.5 \times 10^{19}$ eV. It turned out that 14 of these 16 events were radio emissions from down-going UHECRs, but reflected off the Antarctic ice surface. ANITA takes an advantage of vast detection area ($\sim 10^6\,\mathrm{km}^2$) within a horizon distance of $\sim$ 600 km from the 35 km of high altitude. Although ANITA has great advantage of covering a large detection area, there are several important drawbacks: (1) the flight duration of the NASA Antarctic balloons is typically limited to ∼30 days. The duty factor further reduces to 10 days/year since the flight opportunity for such balloon projects is roughly once in every three years, (2) ANITA's frequency range is 200–1200 MHz, which is optimized for UHE neutrino detection.[5,6] In contrast, UHE cosmic ray induced geo-synchrotron radiation is significantly enhanced at lower frequencies down to 10 MHz.[7–13] Deployment of low frequency antennas to the ANITA payload is difficult due to its weight and space constraints, (3) because the field strength of signal is proportional to 1/R, when it propagates through a long distance to high altitude, only very high energy events can survive and thus lowers event rate, (4) typical altitude of the shower maximum for UHECRs is 10 km, which is much lower than the ANITA's observation point. Only reflected-off signals are detectable except a small fraction of events coming from near the horizon.

Our approach, Taiwan astroparticle radiowave observatory for geo-synchrotron emissions (TAROGE), is to invoke the proven ANITA detection methodology, but places the antennas at the top of high mountains near the ocean. Figure 1 shows the detection concept of TAROGE. This approach resolves all problems of ANITA described above. Thanks to the ideal geology of Taiwan's east coast, where there are numerous mountains as high as 2–3 km in altitude near ocean. At 2 km altitude the horizon-distance is 160 km, which would provide a $1.3 \times 10^4\,\mathrm{km}^2$ detection area as a reflector with a 60° field-of-view. Although the detection area is smaller than ANITA, TAROGE has a great advantage of year-round operation with a high duty cycle, which compensates the area loss. Furthermore, lowering the detection frequency range to 110 MHz (and possibly below) and reducing the detection altitude to 2 km would enhance the signal strength and would therefore allow TAROGE to lower the energy threshold. The sea water is highly reflective for radio frequency (RF); the reflection coefficient is near 100% for the horizontally polarized wave, and

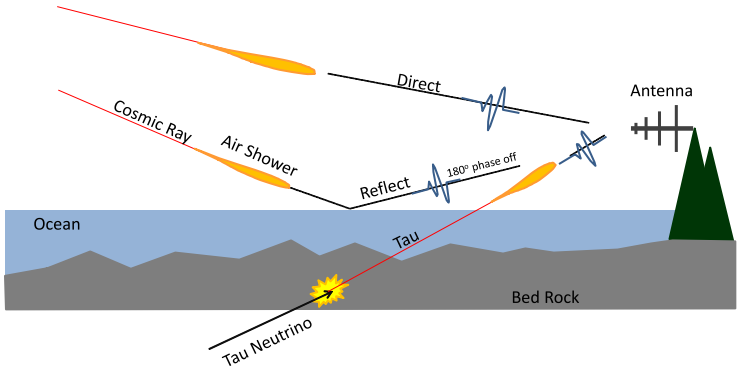

Fig. 1. Detection concept of TAROGE.

higher than 60% for the vertically polarized wave except a small grazing angle. Surface roughness due to ocean wave would be an issue weakening the signal strength. However, this effect is reduced for low frequency range in which the wavelength is longer than the surface roughness for the typical wave condition. TAROGE's receiver configuration that points toward the horizon is sensitive to showers with large zenith angles, which is utilized for UHECRs with energies of $10^{18.5}-10^{19}$ eV. The east coastal region of Taiwan is much less populated than other areas of Taiwan, providing a quieter ambient RF environment. Figure 2 shows power spectra obtained from our initial RF survey at multiple locations in the mountain area of eastern Taiwan. Although many frequency bands appear to be polluted by continuous waveform (CW) noises, there are still fairly quite bands where the noise floors are comparable to thermal- and Galactic-noises. Using RF filters and a trigger system which is only sensitive to coherent signal, Taiwan could be a feasible place for this experiment. This detection technique not only can be applied in Taiwan, but may also be extended to other places with better and quieter RF environments in future.

2. The TAROGE-1 Station

As the first step, in order to demonstrate the detection concept of TAROGE and to perform a long-term noise survey, we built a prototype station, TAROGE-1, in Yongshih Mt. at 1000 m elevation near Heping township, Taiwan, in July 2014. This site had an excellent infrastructure including a good accessibility on a paved road, AC power lines, and a 12 m tall truss tower for mounting antennas. Because of a fact that the site has both views of the open ocean and the township in the field of view, it is almost an ideal location for detailed ambient RF studies with various anthropogenic noise sources near the coast as well as cosmic ray signals. Figure 3 shows the overall structure of the TAROGE-1 station. TAROGE-1 consists of 12 of 5 dBi log-periodic dipole array (LPDA) antennas for 110–300 MHz. A dual polarization configuration, the horizontal polarization (H-pol) and the vertical polarization

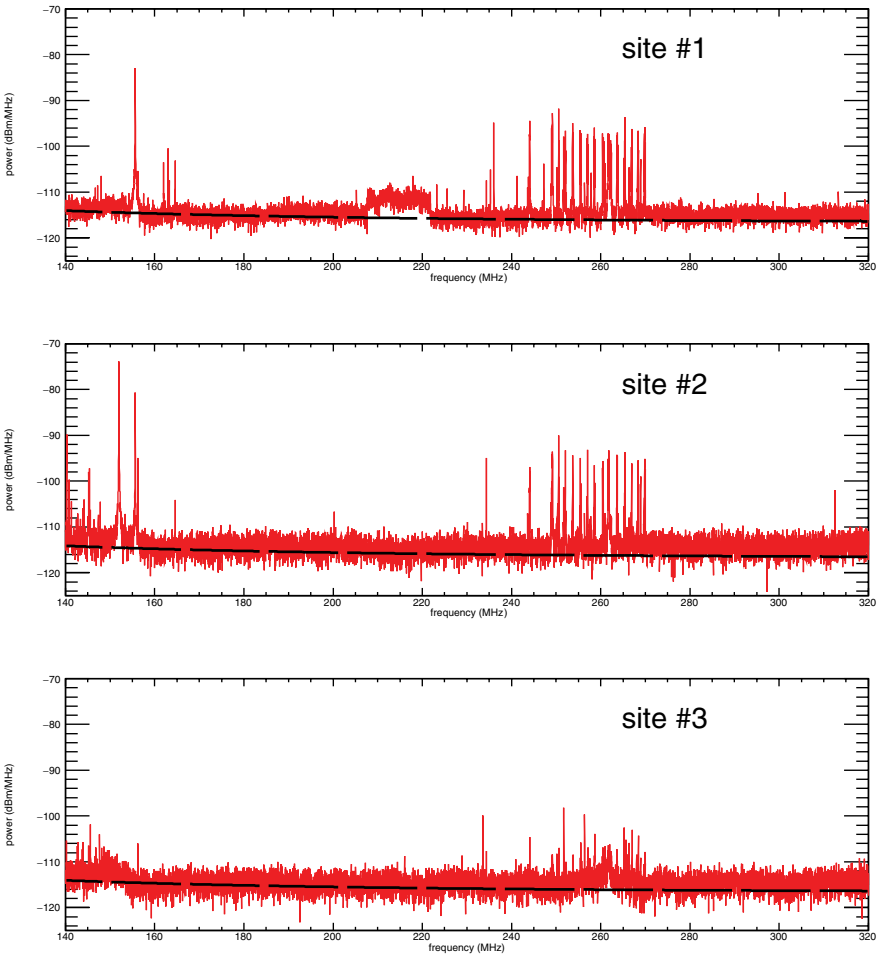

Fig. 2. RF noise spectra in the east mountain area: Data taken in a mountain near ocean (top), in a mountain 10 km away from ocean (middle) and in a deep valley without ocean view (bottom). Dashed lines indicate estimation of the noise floor contributed by thermal- and Galactic-radiations.

(V-pol), is implemented by orientating E-planes of six antennas to the horizontal direction and another to the vertical.

Figure 4 shows the system architecture of TAROGE-1. Received signal in the antenna is fed into the RF front-end before the trigger and digitizer system. The RF front-end consists of a front-end filter, a low noise amplifier (+35 dB), and a second stage amplifier (+30 dB). The RF front-ends are located close to the LPDAs to minimize transfer losses. The signals are transferred via coaxial cables to the data acquisition (DAQ) box where the trigger and digitizer system are placed. The RF signals are split into two paths, the trigger and the digitizer in the DAQ box.

The TAROGE trigger uses the multi-frequency bands coincidence technique, basically similar to ANITA, which provides an effective discriminating power

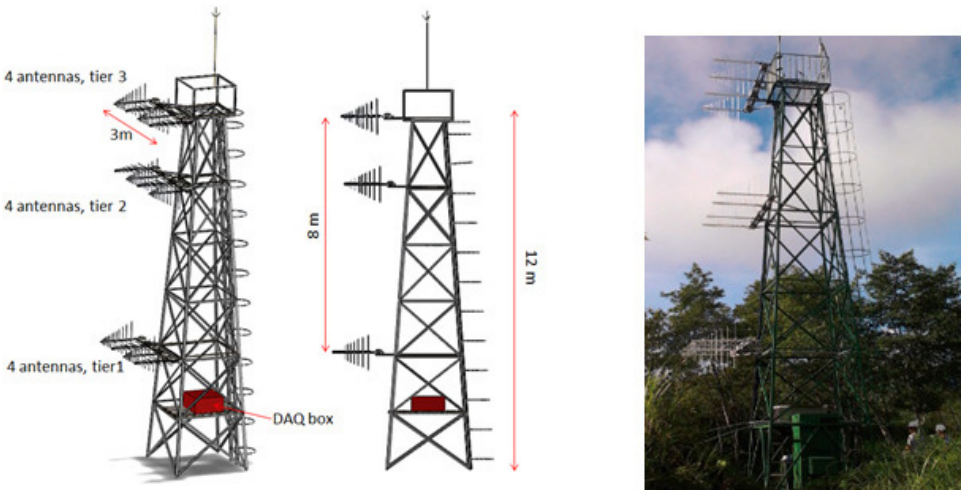

Fig. 3. The TAROGE-1 Station mechanical rendering (left) and figure after the installation completed (right).

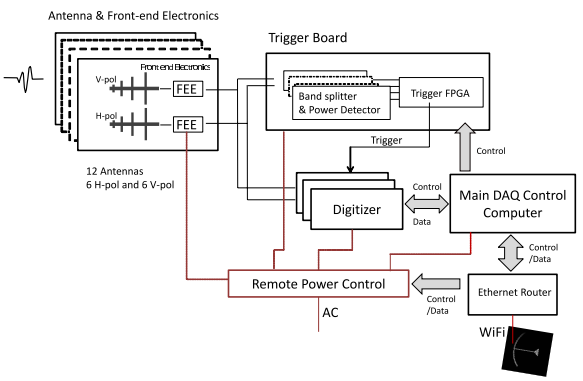

Fig. 4. System architecture of TAROGE-1.

for impulsive geo-synchrotron signals against thermal noises as well as CW anthropogenic-backgrounds. The thermal noise events are further reduced by requiring multiple antennas coincidence. Figure 5 shows the architecture of trigger system. The signal path in the trigger system is fed into four bands; 110–140 MHz, 170–200 MHz, 220–250 MHz and 270–300 MHz. Uncovered frequency regions between the bands are selected to avoid communication CW signals along the east coast of Taiwan. Incident increase of RF power is examined by a power detector and a comparator in each band. Individual thresholds of sub-band can be adjusted by multi-channel DACs through remote commands. The dominated emission power of the geo-synchrotron in Taiwan is V-pol because of a low inclination of Earth magnetic field. However, the Askaryan effect[14,15] in the extensive air-shower still produces a fair amount of power in H-pol.[4] Furthermore, the reflection coefficient

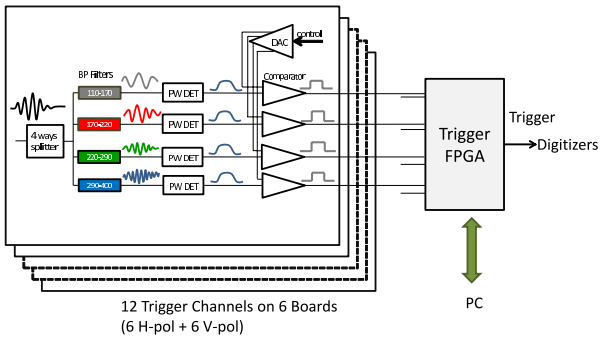

Fig. 5. Schematic diagram of trigger system of TAROGE-1.

of H-pol is much higher than V-pol especially in the low grazing angle which is less than 10°. Therefore, we designed the trigger to perform both in H-pol and V-pol, but independently.

The digitizer system uses affordable commercial digital oscilloscopes with the 300 MHz bandwidth and 8 bit ADCs. We operate the system with 1 GHz sampling rate for a record length of 1 μs. The record length is somewhat longer than the optimal configuration, which causes traffic in data transfer to the main computer, but is limited by the company's firmware. The maximum rate of event readout is ~7 Hz, which is the bottleneck of the TAROGE-1 DAQ. The data size is 50 KB/s (or 4.3 GB/day) after compression. Real-time data transfer and system control is available through the internet. We use a long range Wi-Fi repeater with 24 dBi dish antennas linking between the TAROGE station and the Edu-net at Heping Elementary School in the township. All active elements of the system are placed in Faraday boxes to ensure EMI shielding with shielding power better than −60 dB. Waterproof enclosures are also used to protect electronics and to prevent change of impedance of RF connectors for severe weather conditions.

A precise geometry survey was carried out to measure coordinates of antennas, which is crucial to ensure a good pointing capability. A laser theodolite with an arc-sec angular resolution was used to provide a precision of 1 mm. After completed the installation of station, system validation and calibration were followed using a calibration pulser system which consists of an impulsive pulse generator and a LPDA antenna. The transmitter power was varied using an adjustable attenuator, and polarization angle was varied by changing tip-tilt angle of an antenna mount on a tripod. The pulser signals were sent from multiple locations near the coastal line where its distance to the TAROGE-1 station is 3–5 km. Because the oscilloscope readout reached the saturation rate due to numerous numbers of impulsive noises from the township, triggering on the pulser events was challenging unless a high threshold signal-to-noise ratio (SNR $>$ 10) was required.

Figure 6 (left) displays recorded waveforms of one of the pulser events. The timing calibration was performed using the pulser events. We used the cross-correlation

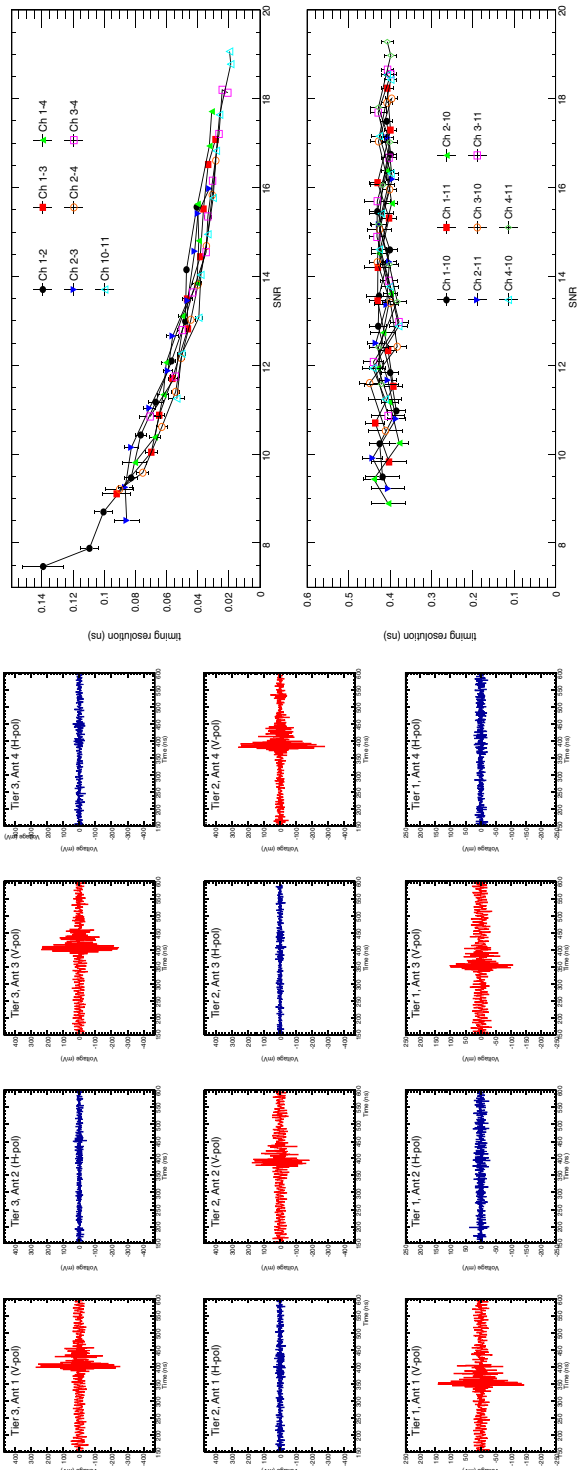

Fig. 6. Left: Pulser event waveforms (V-pol event), Right: Time resolution versus SNR: for channels on the same board (top) and for channels on different boards (bottom).

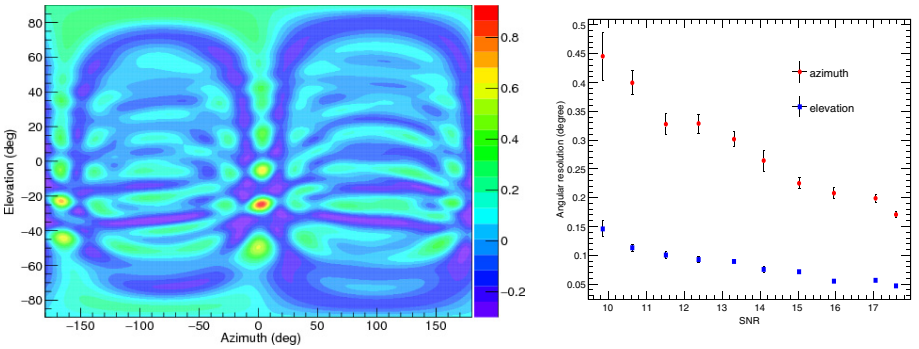

Fig. 7. Left: Interferometry image of the calibration pulser event, Right: Angular resolution versus SNR.

technique[16] to measure arrival time difference between antennas. As shown in Fig. 6 (right), we achieved an excellent timing resolution ∼80 ps for SNR = 10 signals for antenna pairs connected to the same oscilloscope. The antenna pairs in different oscilloscopes has ∼400 ps time resolution which is dominated by the trigger jitter of the oscilloscope.

We use the interferometry imaging method[17] to determine the arrival direction of the incoming RF signal. Figure 7(left) shows an interferometry image obtained from the calibration pulser event. Figure 7(right) shows an excellent angular resolutions, which is better than 0.15° in elevation angle and 0.45° for horizontal angle, are achieved.

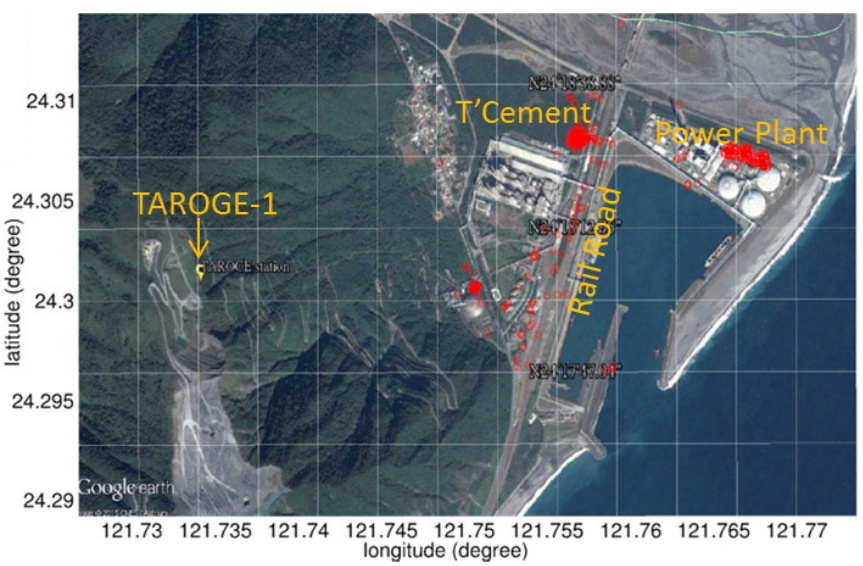

Fig. 8. (Color online) Map of locations of reconstructed impulsive noise events (red mark) superimposed on a map around the TAROGE site.

Figure 8 shows the distribution of reconstructed locations of the detected impulsive noise events in TAROGE-1 data. The event coordinate are determined by extrapolating the arrival directions of signal to the ground level. The result indicates that the most populated event ($> 95\%$) locations are associated to two industrial facilities: one is the cement factory and the other is the power plant. A small portion of events are associated to transportations on the railway and roads.

TAROGE-1 has been operating smoothly since the beginning of August 2014. There are some nonoperating periods during severe weather conditions as like typhoons, power outages due to failure of power line, and maintenances and minor upgrades of the system. The overall duty cycle is more than 65%. The system operated remarkably stable with a duty cycle almost 100% during winter and spring.

3. The TAROGE-2 Station

In December 2015, the TAROGE-2 station was successfully built in the southern part of Yongshih Mt. at 1100 m elevation, located ∼1000 m apart from the TAROGE-1 station. The TAROGE-2 site has a great advantage over TAROGE-1 in terms of the ambient RF noise. While TAROGE-1 faces to the Heping Township in where two big industrial facilities are located, TAROGE-2 faces to the ocean without any anthropogenic noise sources in the field of view. Hualian city is located 30 km away from the site in the south direction, or 100° off from the boresight of antennas, where the gain of antenna drops by more than 25 dB. There are three antenna towers in the TAROGE-2 station, which forms triangular radio array. Figure 9 shows the structure of antenna towers and its allocation. One of the towers (tower #1) was placed on the other platform which is located 5 m higher than the base platform. Two dual-polarized LPDA antennas were mounted in each tower with a 2.5 m spacing. Figure 10 shows a photo of TAROGE-2 station.

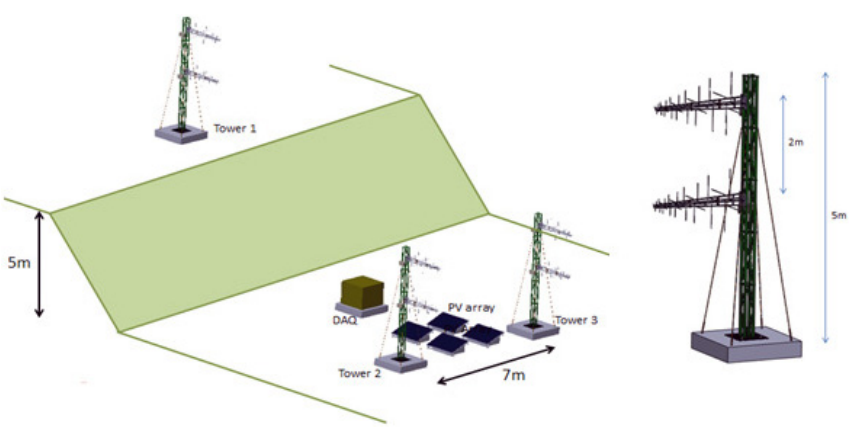

Fig. 9. Rendering of TAROGE-2 station.

Fig. 10. The TAROGE-2 Station after the deployment completed. The Tower-1 is not pictured.

The design of the TAROGE-2 station is conceptually the same as TAROGE-1. However, there are many of remarkable improvements; (1) enhanced antenna gain from 5 dBi to 7 dBi, (2) enlarged bandwidth from 300 MHz to 350 MHz, (3) new design of the trigger board to which is insensitive to temporal appearance of CW noises, (4) improved readout speed by five times allowing upto 40 Hz in DAQ, (5) improved time resolution with a new synchronization technique using the injected sine wave, and (6) improved pointing capability. The TAROGE-2 has a stand-alone power system because the site is located away from the electrical grid. We use a solar photovoltaic (PV) array for the 400 W maximum power.

Like TAROGE-1, the system validation and calibration using the calibration pulser were carried out after the installation completed. TAROGE-2 has been taking data smoothly since late December 2015. A prelimnary analysis of the calibration data shows an improved pointing resolution, 0.1° and 0.05° for the elevation angle and the horizontal angle, respectively. Detailed analyses of the calibration data and physics run data are in progress. The overall duty cycle is about 70% due to the power limit of the PV system. An upgrade using a wind turbine to compensate inefficiency of the PV system during cloudy days is planned for installation in May 2016.

4. Discussions

During 2012–2015, we have successfully completed the construction of two stations, TAROGE-1 for a prototype station which was aimed for systematic studies of RF ambient around eastern high mountain in Taiwan, and TAROGE-2 which was utilized for the cosmic ray detection. The isolated site for TAROGE-2 was found to be a promising location with a wide field of view and the minimal effect of impulsive anthropogenic backgrounds. However, the CW noise from Hualian city

is still a remaining issue which degrades the system sensitivity. In order to minimize the effect of the CW noises, several upgrade plans, such as increased number of receivers with high gain antennas, increased number of frequency bands for the trigger, and exploring the low frequency below 80 MHz are under consideration. The initial simulation study expected an event rate as 45 events/(year·station) at the 1000 m observation altitude with assumptions of the 100% duty cycle and no CW effect. A detailed simulation study with the improved model of the geo-synchrotron emission based on the laboratory measurment[18] is in progress. The extension of TAROGE was funded by the Vanguard program of Ministry of Science and Technology (MOST), Taiwan, to build a total of seven stations in five years.

Acknowledgments

This work has been supported by the pioneer program of MOST, Taiwan. We gratefully thank Taiwan Cement Corporation and Heping Elementary school for their invaluable support.

References

1. Pierre Auger Collab., *Nucl. Instr. Methods A* **798** (2010) 172.
2. LOPES Collab. (H. Falcke *et al.*), *Nature* **435** (2005) 313.
3. ANITA Collab. (S. Hoover *et al.*), *Phys. Rev. Lett.* **105** (2010) 151101.
4. Pierre Auger Collab. (T. Huege *et al.*), *Nucl. Instrum. Methods A* **617** (2010) 484.
5. ANITA Collab. (P. Gorham *et al.*), *Phy. Rev. Lett.* **99** (2007) 171101.
6. ANITA Collab. (P. Gorham *et al.*), *Phy. Rev. Lett.* **103** (2009) 051103.
7. T. Huege and H. Falcke, *Astropart. Phys.* **24** (2005) 116.
8. M. Ludwig and T. Huege, *Astropart. Phys.* **34** (2011) 483.
9. O. Scholten, K. Werner and F. Rusydi, *Astropart. Phys.* **29** (2008) 94.
10. J. Alvarez-Muñiz, *et al.*, *Phys. Rev. D* **86** (2012) 123007.
11. T. Huege, M. Ludwig and C.W. James, *AIP Conf. Proc.* **1535** (2013) 128.
12. D. Heck *et al.*, FZKA Report 6019, Forschungszentrum Karlsruhe (1998).
13. T. Huege, R. Ulrich and R. Engel, *Astropart. Phys.* **27** (2007) 392.
14. G. A. Askaryan, *J. Exp. Theor. Phys.* **14** (1962) 441.
15. G. A. Askaryan, *J. Exp. Theor. Phys.* **21** (1965) 658.
16. ANITA Collab. (P. Gorham *et al.*), *Astropart. Phys.* **32** (2010) 10.
17. ANITA Collab. (A. Romero-Wolf *et al.*), *Astropart. Phys.* **60** (2015) 72.
18. T-510 Collab. (K. Belov *et al.*), arXiv:1507.0729.